environments

Article

Torrefaction of Forest Residues Using a Lab-Scale Reactor

Marta Martins [1], Maria Amélia Lemos [1,*], Francisco Lemos [1] and Helena Pereira [2]

[1] Centro de Recursos Naturais e Ambiente (CERENA), Instituto Superior Técnico, Universidade de Lisboa, 1049-001 Lisbon, Portugal; marta.oliveira.martins@tecnico.ulisboa.pt (M.M.); francisco.lemos@tecnico.ulisboa.pt (F.L.)
[2] Centro de Estudos Florestais, Laboratório Associado Terra, Instituto Superior de Agronomia, Universidade de Lisboa, 1349-017 Lisbon, Portugal; hpereira@isa.ulisboa.pt
* Correspondence: mandal@tecnico.ulisboa.pt

Abstract: Forest residues have been gaining interest as a source of renewable fuels due to their availability and the risks they represent for increasing forest fires. A major drawback for their removal and processing is the cost of transportation, which can be overcome through densification procedures, e.g., torrefaction. To optimize the torrefaction parameters, *Cistus ladanifer* residues from the Portuguese forest were torrefied for 30 min in a lab-scale reactor at 250 and 350 °C. The quality of the torrefied material was assessed, and its energy and mass yields were determined through thermal analysis. The changes in morphological structure occurring during torrefaction were analysed through scanning electron microscopy. When compared to the original biomass, the charcoal obtained at 350 °C had a substantial increase in energy density accompanied by a significant mass reduction. Increasing the mass in the reactor had a positive effect on the energy yield. For the highest mass tested, a mass reduction of around 30% was obtained and a char with no loss in energy content (with a cumulative heat flow (CHF) of 9.0 MJ/kg compared to 5.8 MJ/kg of the original biomass). Modelling of the reactor allowed the analysis of the heat profile required for torrefaction.

Keywords: torrefaction; biomass; mass yield; energy yield; fuels; *Cistus ladanifer*

Citation: Martins, M.; Lemos, M.A.; Lemos, F.; Pereira, H. Torrefaction of Forest Residues Using a Lab-Scale Reactor. *Environments* **2023**, *10*, 202. https://doi.org/10.3390/environments10120202

Academic Editor: Simeone Chianese

Received: 31 October 2023
Accepted: 13 November 2023
Published: 23 November 2023

1. Introduction

In the drive to produce energy from renewable sources, biomass is already a major contributor to renewable energy in Europe [1] and around the world. In the overall energy scenario, the importance of biomass-derived fuels is likely to continue to rise in the context of the decrease in fossil fuels, in the effort to decarbonize [2]. Portugal has a very large potential for the use of biomass as an energy source, in particular of forestry residues, given the large areas of forest plantations and the important forest industries. The removal of forestry wastes is crucial in the context of fire prevention, which is a pending threat, namely during the summer period. According to a study carried out in 2017 [3], the Portuguese forested surface comprises 37.5% of woody areas, 56.1% of shrubs and open woodland, and 6.4% of grazing lands. Shrublands have been increasing, partially due to forest fires and lack of management. Among shrubs and understory vegetation, rock rose (*Cistus ladanifer*) is one of the most important and spreads with an invasive nature. It is a highly combustible material and its flammability makes it a significant fuel for wildland fires, particularly in dry and hot weather conditions.

Although forest management for fire prevention is well established and, in certain cases, mandatory, this task is often not adequately carried out, namely by small holders. Financial incentives for forest residue collection as well as their conversion into valuable solid fuels or to biochar to be used as soil amendment would contribute to improving forest management.

Lignocellulosic biomass is characterized by low bulk density, poor grindability, low calorific value, high moisture content, and poor biological stability. These characteristics

make it difficult and expensive to collect, transport over long distances, and process, in particular for energy production. A way to ensure greater efficiency for transportation and use is the utilization of densification techniques to reduce the volume of material to be transported while retaining its calorific value [4]. Torrefaction is a technology that has been used throughout the ages and is suitable for this purpose since it allows for making the biomass denser, less hygroscopic, and more brittle, among other advantages, without significantly losing the energy content associated with the original biomass. This technique is mainly intended to improve the fuel characteristics of the biomass by altering its physicochemical properties and improving its applicability in thermal conversion processes [5].

Torrefaction is a mild form of pyrolysis consisting of the slow heating of biomass in an inert atmosphere, usually at relatively low temperatures, ranging from 200 °C to 300 °C, and relatively long residence times (torrefaction duration), usually 30–60 min or longer [6]. Upon torrefaction, biomass is converted into charcoal, which has a high energy content, comparable to that of coal, and can be used as a substitute for coal, for example in thermal power plants, to generate electricity and heat [7,8]. During the process of torrefaction, the biomass components (hemicelluloses, cellulose, and lignin) undergo thermal decomposition. In this process, most of the hemicelluloses are thermally degraded, but the extent of decomposition of lignin and cellulose is highly dependent on the temperature and duration at which torrefaction is carried out. The usually accepted decomposition temperature ranges for hemicelluloses, cellulose, and lignin are 200–315 °C, 315–400 °C, and 160–900 °C, respectively [9]. After torrefaction, the moisture (M) and the volatile material (VM) contents of biomass are decreased, whereas its fixed carbon (FC) is increased. Several studies have been conducted on torrefaction using different types of biomass, but the focus has been on woody biomass and on the effect of process conditions on mass loss and the final properties of torrefied biomass for further thermal conversion applications [6,9]. Studies on loblolly pine wood showed that an increase in the torrefaction temperature (250–300 °C) will result in an increase in energy densification of the torrefied biomass, leading to the production of a solid with increased carbon content and a decrease in oxygen and volatiles [10]. In preliminary studies performed on the torrefaction of *Cistus multiflorus* branches, we observed that an increase in torrefaction temperature (200–350 °C) and reaction time (30–90 min) led to a reduction in both mass and energy yields, but, since the energy yield reduction was much lower than that of the mass yield, a very significant increase in energy density of the charcoal occurred [11]. This type of observation can also be found for other types of biomass [12]. For example, bamboo torrefied at 220, 250, and 280 °C during 60 min enhanced its combustible properties [13]. It should be stressed that, from a practical point of view, and considering that a large amount of biomass is to be treated at the industrial level for solid fuel production, a short process duration is desired, while achieving the target weight loss.

The main objective of the present work is to study the torrefaction process and the thermochemical properties of the charcoal produced from *Cistus ladanifer* biomass obtained as forest underbrush waste. The torrefaction process can contribute to forest management and prevent fires by valorising the waste and, thus, promoting its collection and reuse. Furthermore, if the torrefaction process is carried out close to the collection site, for example, by using a mobile system, it will allow the reduction in the amount of waste that has to be transported and, at the same time, provide a stabilisation of the biomass. Changes in surface structure, solid, and energy yields were analysed.

Since it is crucial to understand the occurring phenomena in order to develop a suitable process to carry out the torrefaction process, a kinetic analysis was performed through combined thermogravimetry and differential scanning calorimetry. As a result, a combined kinetic model was developed to understand the thermochemical transformations under nitrogen and air, which can help in both pyrolizer and gasifier design.

The goal, in terms of solid fuel production, is to ensure a significant reduction in mass, which is of significant importance to lower transportation costs while maintaining as much as possible of the calorific value of the original sample. Although this study focuses on the

calorific value of the charcoal produced, other applications can be envisaged, such as its use for soil improvement. Moreover, it will contribute to a better economic framework for forest understorey management, thereby allowing for a more efficient fire prevention by removing highly combustible materials, while generating a valued energy product.

2. Materials and Methods

2.1. Sampling

Cistus ladanifer branches were harvested in the southern region of Portugal (Alentejo) from the understory of a sparse forest. The whole plants were fractionated to separate the stem and branches from the leaves and flowers. Only the woody stems and branches were used in this study, which were stored in individual lots at room temperature (25 °C) until processing. For the testing experiments using biomass samples until 6 g, the branches were manually cut into 2 cm long pieces. For chemical analysis and for experiments with biomass samples over 6 g, the branches were triturated in a blade rotor Retsch 2000 with a sieve output of 2 microns of particle size.

2.2. Biomass Characterization

The chemical composition of the forest biomass was analysed through the sequential determination of extractives, lignin, and polysaccharide content. The inorganic content was quantified as ash [14]. Extractives were determined through successive Soxhlet extractions with pure solvents with CH_2CL_2 (Honey-well, Lisbon, Portugal, ≥99.9%), C_2H_5OH (José Manuel Gomes dos Santos, Lda, Lisbon, Portugal, 96%), and H_2O Millipore, according to the procedure described in the literature [15]. Klason lignin was determined on the extracted sample through acid hydrolysis with a solution of 72% in H_2SO_4 (Chem-Lab, Lisbon, Portugal, 95–97%) [16]. The acid-soluble lignin was determined in the filtrate through UV spectroscopy at 206 nm [17]. Total lignin was determined as the sum of the Klason and acid-soluble lignins. The remaining acid solution was kept for sugar analysis using high-performance liquid chromatography with pulsed amperometric detection (HPLC/IC-PAD) (DIONEX ICS 300). The polysaccharides were estimated by the content in neutral and acid monosaccharides (arabinose, xylose, galactose, mannose, glucose, and galacturonic acids) as well as acetic acid in the hydrolysate obtained from the lignin determination.

Proximate analysis was estimated using the TG data for pyrolysis run up to 800 °C with a heating rate of 10 °C/min, combined with a combustion run of the raw material at the same conditions.

The thermal behaviour of the biomass samples was also analysed through combined TG/DSC both under air and under nitrogen.

2.3. Torrefaction in Lab-Reactor System

A Schlenk-type glass vessel (Scheme 1) of around 0.1 L was placed in an oven for which the temperature was controlled at predefined levels. The reactor was initially flushed with N_2 to ensure a suitable atmosphere in the reactor for torrefaction reactions. Different amounts of biomass samples were introduced in the reactor for the torrefaction experiments. The temperature in the oven was raised, with a heating rate of 10 °C min^{-1}, up to the desired set-point temperature and maintained, in each case, at that temperature for 30 min. The reactor was operated in a semi-continuous mode, allowing all volatiles to exit the reactor; the liquid products were collected above the reactor, after condensation in a condenser, and the gaseous products were collected in a gas burette. After the run, the system was cooled down and the solid was weighed and stored for characterization using thermogravimetric analysis and microscopy techniques.

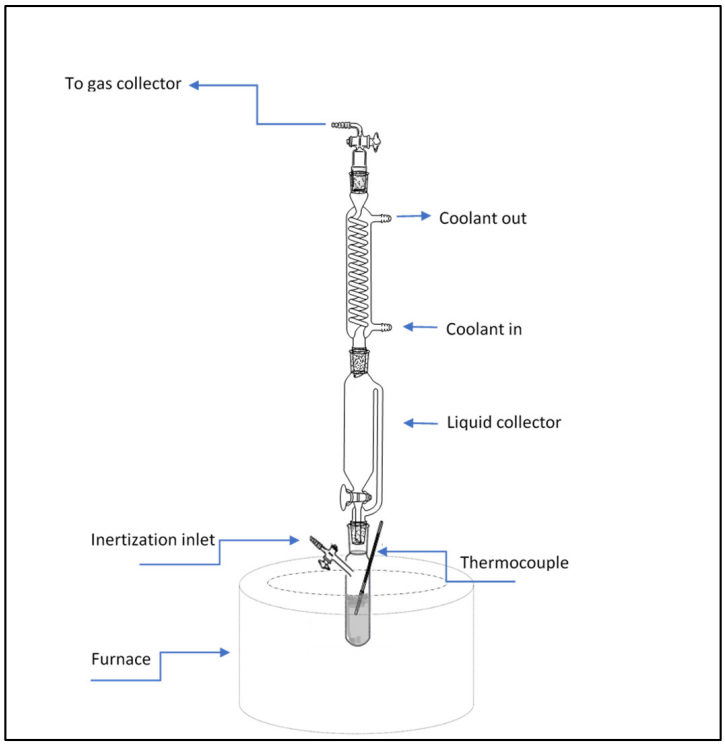

Scheme 1. Lab-scale reactor.

2.4. Thermal Analysis through TG/DSC

Thermogravimetric (TG) analysis of the *Cistus ladanifer* samples was performed in a TA Instruments SDT 2960 with simultaneous differential scanning calorimetry (DSC) at a heating rate of 10 °C min^{-1}. The equipment allowed us to obtain the weight and the heat involved in the processes that were occurring. Derivative thermogravimetric (DTG) data are represented as the symmetric mass loss. In a typical run, an approximately 10 mg sample was weighed and placed in a quartz crucible.

The runs were carried out either under a flow of 0.09 g/min of nitrogen (pyrolysis) or 0.10 g/min of air (combustion). Both the raw and the torrefied material were subjected to runs under nitrogen or air, starting at 40 °C and heating up to 800 °C at a heating rate of 10 °C min^{-1}.

To analyse the impact of torrefaction temperature on the produced charcoal, additional experiments were carried out by heating the samples to different temperatures, also using a 10 °C min^{-1} heating rate, and maintaining the temperature for a period of time.

2.5. Charcoal Characterization

The solids obtained at the end of the torrefaction (charcoal) in the bench reactor were collected and analysed using TG/DSC to evaluate their thermochemical behaviour and estimate their calorific value.

Proximate analysis was performed using the TG data for pyrolysis and combustion experiments of each torrefied material.

Mass (*MY*) and energy (*EY*) yields were calculated as follows:

$$MY = \frac{Weight\ of\ torrified\ biomass}{Weight\ of\ raw\ biomass} * 100 \quad (1)$$

$$EY = MY * \frac{CHF\ torrified\ biomass}{CHF\ raw\ biomass} \quad (2)$$

Proximate analysis was performed to determine moisture, volatile material, fixed carbon, and ash. To compare the calorific value of raw material and of the torrefied biomass

samples, the cumulative heat flow (CHF) was computed, which was estimated, using the DSC signal, from the runs under air. This parameter corresponds to the integral under the DSC curve that gives the amount of energy released when biomass is fully combusted.

The microstructure and the morphology of raw and torrefied material were inspected using a scanning electron microscope (SEM) Hitachi S-2400 (Hitachi, Tokyo, Japan) to acquire cross-sectional surface images. The instrument was operated in high-vacuum mode, and under an accelerating voltage of 20 kV.

2.6. Kinetic Analysis

The kinetic parameters for pyrolysis and combustion of *Cistus ladanifer* biomass were estimated with the assumption of a first-order reaction and using the following equations (Equations (3) and (4)).

$$\frac{dW_i}{dt} = -k_x(T).wi \tag{3}$$

$$k(T) = k_{ref}\ exp\left(-\frac{E_a}{R}\left(\frac{1}{T} - \frac{1}{T_{ref}}\right)\right) \tag{4}$$

where $k(T)$ is the temperature-dependent kinetic constant, w is the fractional weight of the sample at time t, k_{ref} is the kinetic constant reference, E_a is the activation energy (kJ/mol), R is the gas constant, T is the sample temperature, and T_{ref} is the reference temperature.

3. Results

The experiments were planned so that the impact of the torrefaction on the heat content of the samples was systematically analysed. The torrefaction experiments were conducted in the bench-scale reactor and the solid torrefied obtained was subsequently analysed in the thermal-analysis equipment.

The chemical composition of the original samples, as well as their thermochemical behaviour, were analysed to compare them with the torrefied material.

3.1. Sample Characterization

Table 1 shows the chemical composition and proximate analysis of the *Cistus ladanifer* biomass branches used in this study.

Table 1. Summative composition of the *Cistus ladanifer* branches used in this study. For comparative purposes, the chemical composition from another study on *C. ladanifer* [18] as well as that of white broom (*Cistus multiflorus*) branches, from Portugal, are also shown [19]. M, VM, FC represent the moisture, volatile material, and fixed carbon contents of biomass, respectively.

Chemical Composition	***C. ladanifer* (This Work)**	***C. ladanifer* [18]**	***C. multiflorus* [19]**
Ash%	2.2 *	4.1	1.2
Total extractives%	18.2	31.9	11.8
Lignin total%	21.5	18.6	25.0
Klason lignin%	19.1	16.8	
Soluble lignin%	2.4	1.74	
Polysaccharides%	36.6	45.4	62
Proximate Analysis			
M%	4.8		
VM%	86.5		
FC%	5.6		
Ash%	3.0 **		
CHF (MJ/kg)	5.8		

Note: determined through chemical * and thermal analysis **.

The chemical composition of the *Cistus ladanifer* biomass is similar to that obtained in a previous study [18], showing a low amount of ash, a high extractive content, and a low lignin content. The differences between the two *Cistus ladanifer* studies are attributed to the natural variability in biomass samples, in particular due to differences in collection conditions.

The sample was also characterized through proximate analysis to assess moisture, volatile material, fixed carbon, and ash content. The results presented in Table 1 were obtained from TG/DSC data from pyrolysis and combustion experiments of the raw material, and are in good agreement with the literature. Fixed carbon and the volatile matter of ligneous biomass are typically in the ranges of 0.5–20 wt% and 67–88 wt%, respectively, whereas they are 46–92 wt% and 0.9–50 wt% in coal, respectively [20]. Amutio and co-workers reported similar values (10.3 and 80.0 wt% for FC and VM, respectively) for biomass composed of a mixture of 50% of *Cistus multiflorus* and 50% of *Spartium junceum* [21]. The amount of moisture is not very significant as it heavily depends on the collection and storage conditions, but the fact that it is low is relevant for thermochemical processes. The presence of significant amounts of fixed carbon is also very relevant in the context of the production of solid fuels from the biomass under consideration. On the other hand, the differences in ash content in the performed chemical and thermal analysis can be attributed to differences due to the natural variability of biomass.

Thermal analysis is also a good approach to characterize heterogeneous organic materials like forest biomass residues, because it can provide insight into the different components that are present. In this way, thermogravimetric analysis of *Cistus ladanifer* under nitrogen (for pyrolysis) and under air (for combustion) was performed (Figures 1–4) at 10 °C/min.

Figures 1 and 2 show that both under nitrogen and under air, the process starts with the evaporation of moisture up to around 100 °C. At around 240 °C, a significant mass loss occurs, regardless of the atmosphere under which the process takes place, and it should fully correspond to the beginning of the pyrolysis process. The degradation then diverges, depending on the atmosphere. Under nitrogen, a maximum weight loss occurs at around 330 °C, which is characteristic of hemicelluloses and cellulose decomposition, followed by a slower degradation process that extends to higher temperatures and that can be attributed to lignin decomposition [22]. In Figure 2, corresponding to the experiment under air, after the initial moisture loss peak, several broad peaks are overlapped, which can be attributed to the combustion processes of the different components, either directly or through the combustion of volatiles that are produced using pyrolysis processes. The amount of residue after the run under nitrogen, which is significant, mostly corresponds to the fixed carbon, as no significant amount of ash was observed in the degradation under air. The biomass decomposition under nitrogen or air can be described as starting with a similar process at lower temperatures, between 130 and 250 °C, followed by a set of different steps at higher temperatures, between 250 and 500 °C, which, in the case of the reaction under nitrogen, are the thermal decomposition of the more recalcitrant species and, under air, correspond to combustion processes as it is clear when we look at the heat flow signal from the DSC.

In the DSC signal under inert atmosphere (Figure 3), only endothermic peaks can be observed; the first one corresponds to the drying process and is also present in the experiment under air. As expected, the behaviour differs for higher temperatures. In the case of the run under air (Figure 4), there is an important release of energy as the temperature increases, corresponding to the different mass loss peaks observed in Figure 2; three exothermic peaks are observed at 312, 440, and 484 °C. The first and second peaks could be related to the energy released through the combustion of cellulose and hemicelluloses, and the third peak could be related to the energy released through the decomposition of the fixed carbon and residual lignin oxidation. This behaviour is comparable to other published results. For example, the analysis of four types of wood biomass (beech, willow, alder, spruce) also presented three main exothermic peaks at, ca., 280–310 °C, ca., 355–365 °C, and, ca., 410–430 °C, respectively [23]. The observed differences are attributable to the different experimental conditions and sample properties.

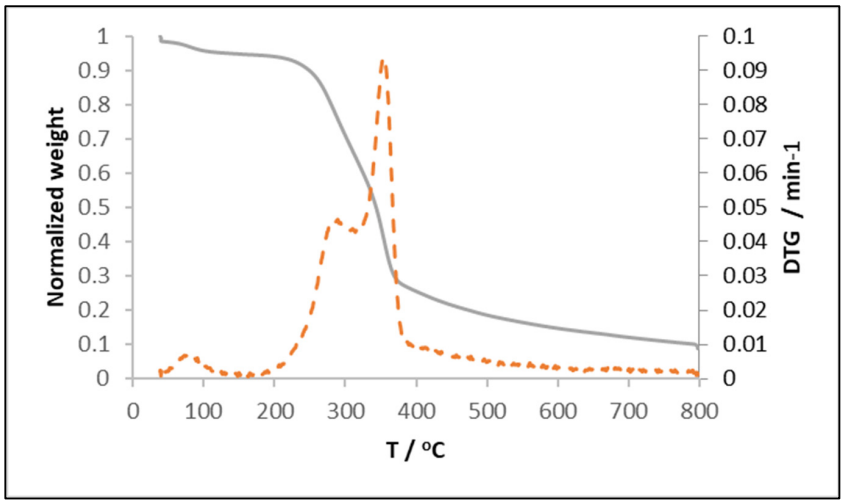

Figure 1. TG (full line) and DTG (dashed line) profiles of *Cistus ladanifer* biomass under nitrogen.

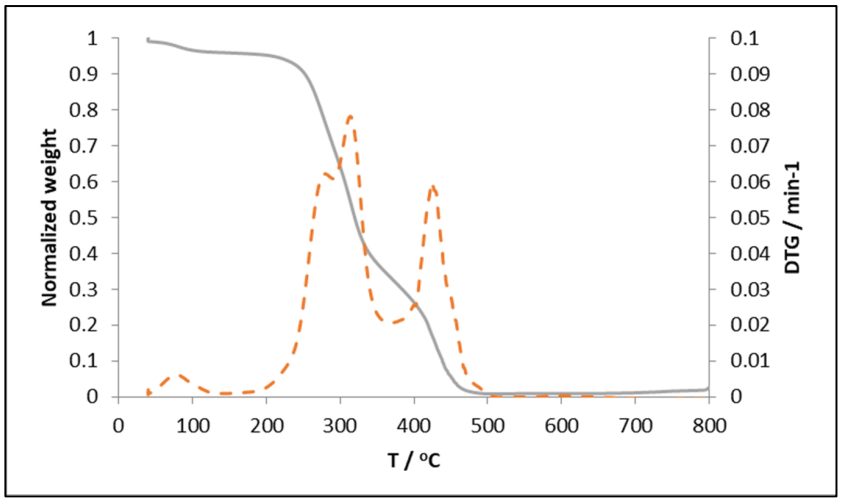

Figure 2. TG (full line) and DTG (dashed line) profiles of *Cistus ladanifer* biomass under air.

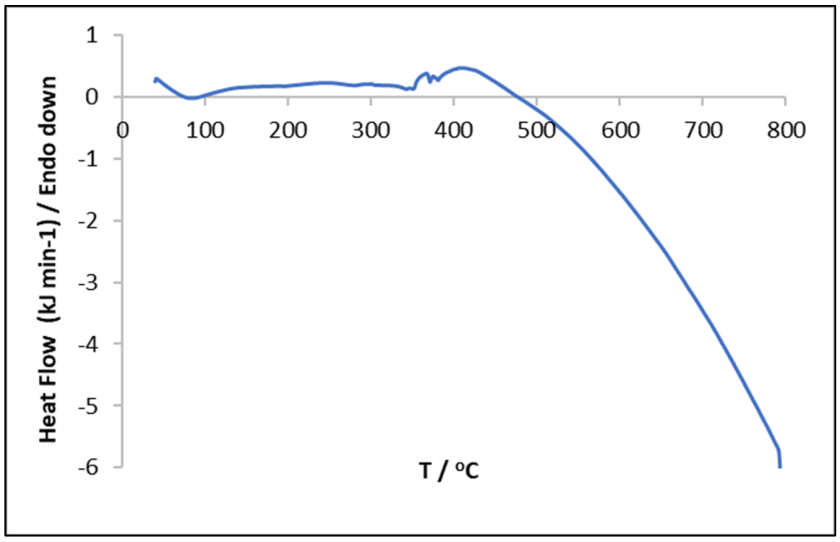

Figure 3. DSC profile of *Cistus ladanifer* biomass under nitrogen.

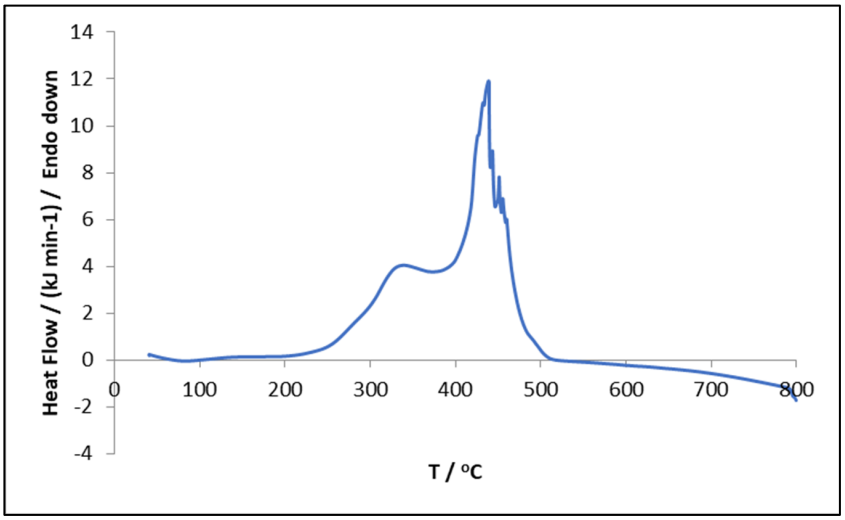

Figure 4. DSC profile of *Cistus ladanifer* biomass under air.

3.2. Thermal Analysis to Evaluate the Influence of Torrefaction Temperature

The extent of the lignocellulosic material decomposition and the way it progresses towards the products depend on the temperature at which the process occurs [24]. To assess the torrefaction process, the samples were heated up to two temperatures (250 °C and 300 °C), which were maintained for 30 min in the TG/DSC apparatus. After the torrefaction procedure, the samples were cooled and a run under air was carried out to analyse the combustion characteristics of the torrefied material and allow the estimation of the CHF (Table 2).

Table 2. Weight loss observed during the torrefaction process of *Cistus ladanifer* biomass at 250 °C and 350 °C during 30 min carried out in the TG/DSC and CHF of the corresponding torrefied material.

Weight Loss in the Torrefaction Process %	Weight Loss in the Torrefaction Process %	CHF % of the Torrefied Material (MJ/kg)
Original	-	5.8
250 °C	22.4	9.7
350 °C	58.0	13.9

The mass loss significantly increased for the higher torrefaction temperature, due to the drying process and the decomposition of macromolecular components of biomass, such as hemicelluloses and cellulose. The cumulative heat flow also increased as the torrefaction temperature increased; the energy density more than doubled in relation to the original biomass and the highest value was achieved for the highest torrefaction temperature comparatively with the CHF of raw biomass. The energy yield, however, was highest for the less severe torrefaction conditions, with values above 100%, indicating that at least part of the energy that was supplied to the sample in the torrefaction process was actually stored in the torrefied material.

3.3. Bench-Scale Reactor

Torrefaction was also carried out at two different temperatures (250 °C and 350 °C) using the bench-scale reactor described above using different masses (from 2 g to 26 g) of *Cistus ladanifer* biomass. Subsequently, the mass and energy yield of each charcoal produced as well as its main characteristics were determined for each torrefaction condition.

Figure 5 depicts the thermal analysis, under air, of the three charcoal samples obtained from the reactor torrefaction process at 350 °C, starting with 2, 4, and 6 g of biomass. The degradation profile is always similar.

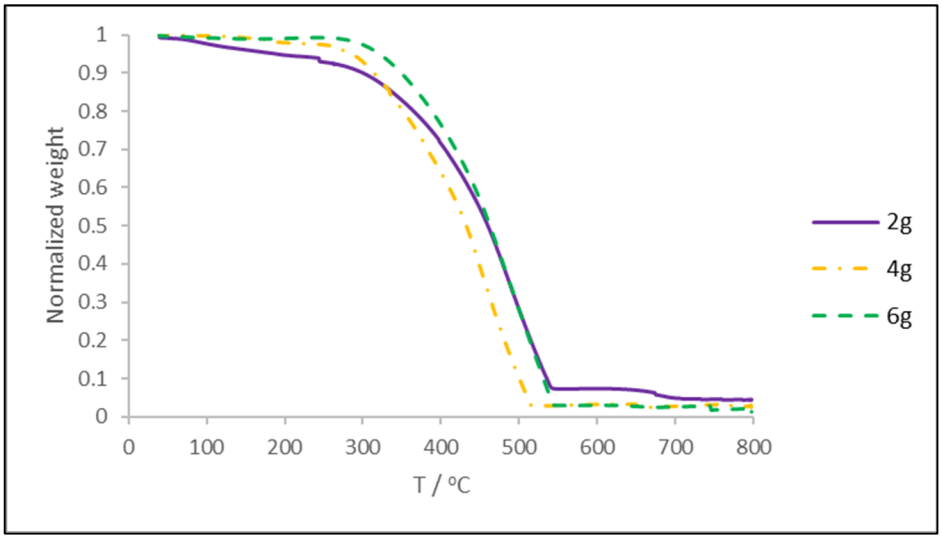

Figure 5. TG profile for the combustion of three torrefied *Cistus ladanifer* samples, obtained in the bench-scale reactor at 350 °C during 30 min.

From the TG profiles of the combustion of the torrefied material at 350 °C, it is possible to see that the combustion onset temperature gradually increases for the charcoals that were obtained from higher starting amounts of biomass.

Figure 6 shows the heat involved in the combustion of the charcoal that was produced at 350 °C for 30 min. Exothermic peaks were observed in the DSC profile, characteristic of combustion of the three major components of lignocellulosic biomass.

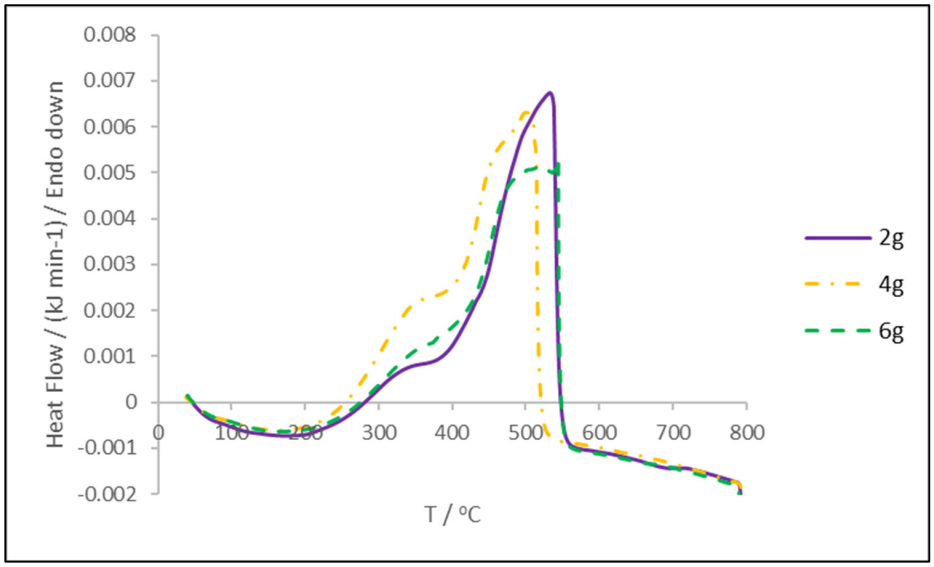

Figure 6. DSC profile for the combustion of the three torrefied *Cistus ladanifer* samples, obtained in the bench-scale reactor at 350 °C during 30 min.

However, comparing Figures 5 and 6 with Figures 2 and 4, which correspond to the original biomass, significant differences are observed, in particular for the samples obtained with the highest amount of biomass in the reactor. There is no water-loss peak at low temperature, consistent with the fact that the charcoal is much more hydrophobic than the original biomass, and the mass loss is now concentrated at higher temperatures, which is consistent with an extensive decomposition of the cellulose and hemicellulose components.

Figure 7 illustrates, for the two torrefaction temperatures, the influence of biomass quantity placed into the bench-scale reactor on the mass and energy yields and on the composition of the torrefied material obtained from the torrefaction of *Cistus ladanifer* biomass.

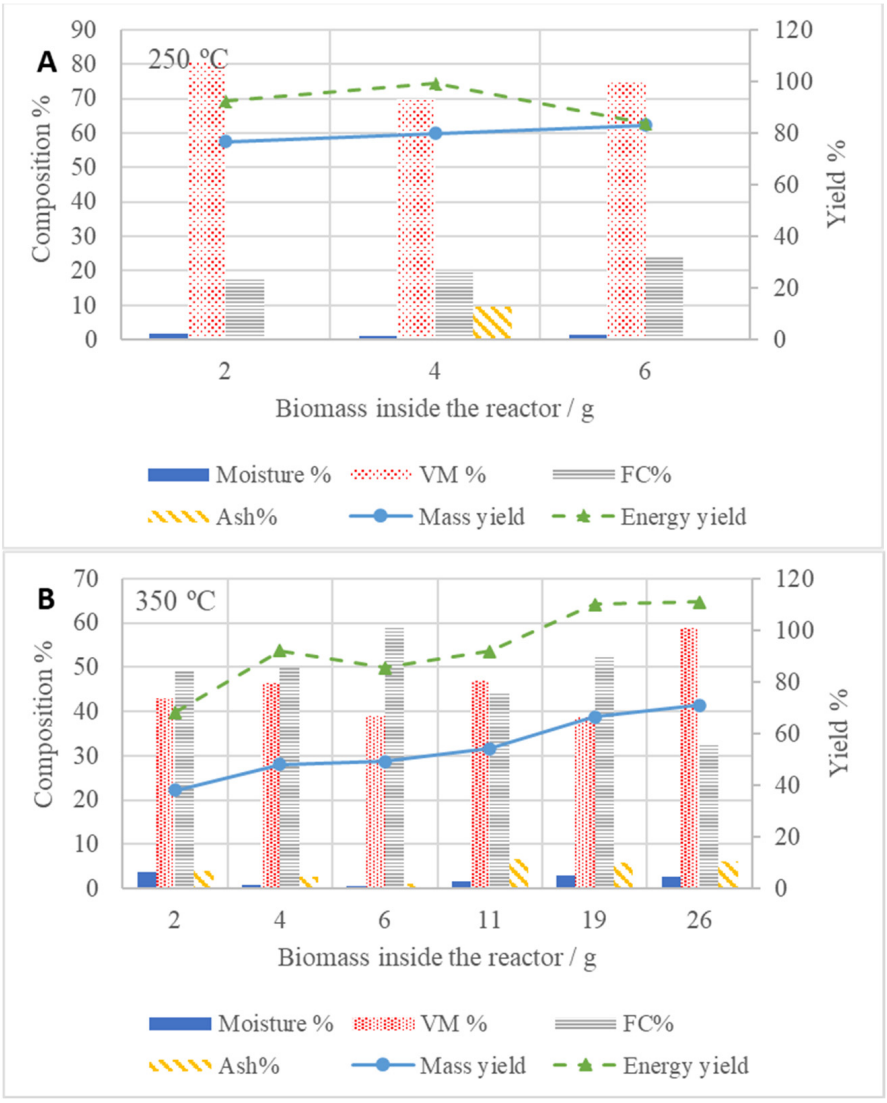

Figure 7. Effect of biomass quantity on energy and mass yields (right axis) and torrefied composition (left axis) for a 30 min torrefaction of *Cistus ladanifer* biomass at 250 °C (**A**) and 350 °C (**B**).

The results obtained show that torrefaction decreases the amount of moisture and volatile matter and significantly increases fixed carbon.

For the lower amounts in the reactor, both the mass and energy yields tend to decrease with the increased severity of the torrefaction process, when going from 250 to 350 °C, although, as expected, the decrease in mass (ca., 50%) is much more significant than the decrease in energy content, which induces a significant increase in CHF.

It is also noteworthy that, for the higher torrefaction temperature, the increase in the amount of material in the reactor induces a significant increase in the energy yield, sometimes reaching values above 100%, indicating that at least a part of the energy that is input to the process is actually stored in the charcoal, while also achieving a significant decrease in the mass of the sample, although the mass yield also increases with the increase in mass.

This accomplishes the general objective of the torrefaction process as it corresponds to a significant decrease in the mass of the sample while retaining most of the energy content,

in some cases almost all of the original energy content or even a small added amount (Table 3). At higher torrefaction temperatures, there is a significant decrease in the mass of the material, maintaining the overall heat content of the sample. This is more noticeable for the runs where more material was processed, as can be seen in Table 3, where higher quantities of biomass were tested for torrefaction conditions at 350 °C. These studies were performed to evaluate the heat and mass transfer processes involved in the torrefaction process. A good impact on the energy yield was observed as the mass inside the reactor increased. Moreover, it is known that the energy density increases through torrefaction. After torrefaction at optimum conditions of 250 °C for 30 min, corncob achieved an energy density of 1.48, which is close to the value obtained in this work when 6 g of raw material was used (1.01) [25].

Table 3. Mass and energy yields and CHF obtained for 30 min torrefaction of *Cistus ladanifer* biomass at 250 °C and 350 °C on the bench-scale reactor and on the TG (10.5 mg).

Temperature °C	Amount kg	Mass Yield %	Energy Yield %	CHF (MJ/kg)
Original		**-**	**-**	**5.8**
250 °C	TG	77.6	129.8	9.7
	0.002	76.7	92.3	6.9
	0.004	79.8	99.2	7.2
	0.006	83.1	83.7	5.8
350 °C	TG	42.0	100.6	13.9
	0.002	38.0	68.4	10.4
	0.004	48.0	92.2	11.1
	0.006	49.2	85.6	10.1
	0.011	54.3	91.9	9.8
	0.019	66.4	110.1	9.6
	0.026	70.9	111.0	9.0

These results are promising and are consistent with observations from other authors on different biomass samples (willow, beech, larch, straw [26]; eucalyptus residues [27]; pine wood chips [28]; cotton gin [29]; wood block [30]; herbaceous biomass [31]; Norway Spruce [32]), where the mass yield of biomass is usually in a range from 24 to 95%, while the energy yield ranges from 29 to 98%, after the torrefaction process [6,12]. It is noteworthy that CHF obtained in the bench-scale reactor is always lower than the values obtained in the small-scale TG runs, probably due to the easier heat and mass transfer in the TG crucible, where the torrefaction occurs under a flow of nitrogen, whereas, in the reactor, there is an almost static atmosphere as only light volatile components are allowed to leave the reactor. Also, energy yields above 100% are obtained under certain conditions. This result is likely achieved due to the design of the reactor that retains the heavier volatile species inside, inducing an increase in the heat content of the charcoal.

It is also noteworthy that in the case of the runs at 350 °C and with a higher mass of the samples, the samples were not crushed, to better simulate what could be done if this method was to be used in field conditions. The results indicate that the use of the material as such was not deleterious to the final objective of having a decrease in mass while keeping the energy yield high.

Other works indicate that the calorific value of biomass linearly varies with mass loss, implying that a reduction in solid yield increases the energy content of the material [33,34]. In the case of our study, a linear trend between CHF and mass loss is also observed, as can be seen in Figure 8. The heat content values are also comparable with those reported for lignite coal (<17.4 MJ/kg) [35].

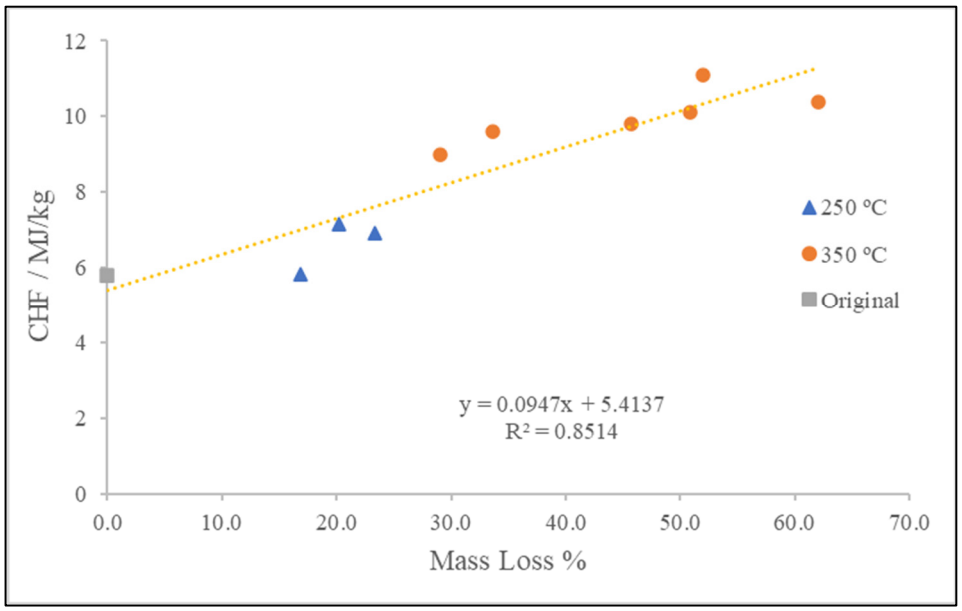

Figure 8. Effect of the mass reduction on the CHF of torrefied *Cistus ladanifer* samples pyrolysed for 30 min at 250 °C and 350 °C in a bench-scale reactor. The CHF value for the original (non-torrefied *Cistus ladanifer* sample) is also shown for comparison.

These results also indicate that the relation holds regardless of whether the sample is crushed or not.

In this work, the results have shown that torrefying 26 g of *Cistus ladanifer* biomass at 350 °C for 30 min leads to a mass reduction of around 30%, yielding a char that contains 111% of the initial energy content (with a CHF of 9.0 MJ/kg when compared to 5.8 MJ/kg of the original biomass). As indicated, energy yields above 100% imply that the charcoal actually retains some of the energy that was supplied to the torrefaction process, acting as an energy storage material.

3.4. Thermal Analysis of Torrefied Material

To allow for a more detailed analysis of the torrefied materials, the samples obtained at 350 °C for 2, 4, and 6 g were subject to thermal analysis under air and the results were modelled using a lump approach with five degradable components and ash; all reactions were considered to be first-order in relation to the respective component. The same five components were used for all the samples, to ensure comparability for all the results, and the kinetic parameters were optimised through simultaneous fitting to all the thermograms, including that for the original biomass. The fraction of each of the five components was obtained independently for all the samples.

The main kinetic parameters of the five components are shown in Table 4, together with the corresponding fractions estimated for each of the torrefied materials and for the original biomass.

From the results obtained in Table 4, we can tentatively assign the first component as moisture; the second and third to cellulose and hemicelluloses, respectively; and the fourth, fifth, and sixth to different recalcitrant materials and ash, presumably different moieties of lignin or fixed carbon.

The results for the original biomass are consistent with this assignment as the fourth component is around 40%, which is comparable to the amount of lignin shown in Table 1. The distribution estimated for the torrefied materials show that there is a significant reduction in moisture content, as expected since the torrefied material is more hydrophobic, and also that the two components associated with cellulose and hemicellulose have sharp reductions.

All torrefied materials show a significant increase in the fourth and fifth components, which can be associated with carbonised material.

Table 4. Kinetic parameters (k_{ref}—kinetic rate constant at the reference temperature of 573.15 K, E_a—activation energy, and T_{max}—temperature of the maximum reaction rate) and fractions of the five components plus ash model used to model the thermograms under air of the original biomass and the torrefied materials obtained in the semi-batch reactor at 350 °C and different masses.

	Component					
	1	**2**	**3**	**4**	**5**	**6**
k_{ref} (min^{-1})	584	4.06	0.262	1.13×10^{-3}	4.3×10^{-6}	-
E_a (kJ/mol)	5.8×10^4	1.6×10^5	1.2×10^5	6.8×10^4	2.0×10^5	-
T_{max} °C	88	270	311	433	514	-
$x_{original}$	0.04	0.12	0.40	0.44	0	0
x_{2g}	0.04	0.01	0.04	0.53	0.32	0.06
x_{4g}	0.01	0.00	0.06	0.80	0.1	0.02
x_{6g}	0.01	0.00	0.02	0.59	0.37	0.02

3.5. Bench-Scale Reactor Modelling

To gain further insight into the way the reactor works, a simple model was used to analyse the reactor information, based on an energy balance on a lab-scale reactor, which is a semi-batch reactor. The following general equation was used, where all the heat losses from the reactor were gathered in a single term:

$$(M_{empty\ reator}\overline{C_{p(empty\ reactor)}} + M_{sample}\ \overline{C_{p(sample)}})\frac{dT_{reactor}}{dt} = UA(T_{oven} - T_{reactor}) + (-\Delta_r H)r - L(T_{reactor} - T_{room}) \quad (5)$$

where $T_{reactor}$, T_{oven}, and T_{room} are, respectively, the temperature of the reactor, the temperature of the oven in which the reactor is placed, and the room temperature (18 °C); L is the coefficient of thermal losses (kJ/K/min); M is the mass (kg); Cp is the calorific value (KJ/kg/K); $\Delta_r H$ is the heat of reaction (kJ/kg); and UA is the global heat transfer coefficient (kJ/K/min).

To parameterize the model to the specific reactor that was being used, the values for L, UA, $M_{empty\ reactor}$, and $C_{p(empty\ reactor)}$ were estimated from blank experiments carried out with an empty reactor (see the curve for the empty reactor in Figure 9).

Although solving Equation (5) requires the knowledge of the rates of the reactions taking place inside the reactor, it is possible to use this equation as a way to analyse the reactor as a calorimeter and compute the heat flow to the sample inside the reactor; this energy includes the amount of energy that is required to heat the sample, as well as the energy supplied/produced by the reactions occurring in the reactor. Reorganizing Equation (3), we obtain

$$Heat\ Flow = M_{sample}\ \overline{C_{p(sample)}}\frac{dT_{reactor}}{dt} - (-\Delta_r H)r = UA(T_{oven} - T_{reactor}) - L(T_{reactor} - T_{room}) - M_{empty\ reactor}\ \overline{C_{p(empty\ reactor)}}\frac{dT_{reactor}}{dt} \quad (6)$$

From this equation and using the temperatures that were obtained in the experiments performed with biomass, the heat flow was computed.

Figure 9 shows the temperature profile obtained for the reactor with 2 g of biomass, as well as the profile for the empty reactor for comparison. With the sample inside, the temperature increases much more slowly since energy is needed to heat the materials, and because of the mostly endothermic processes occurring inside, like water evaporation and the pyrolysis reactions.

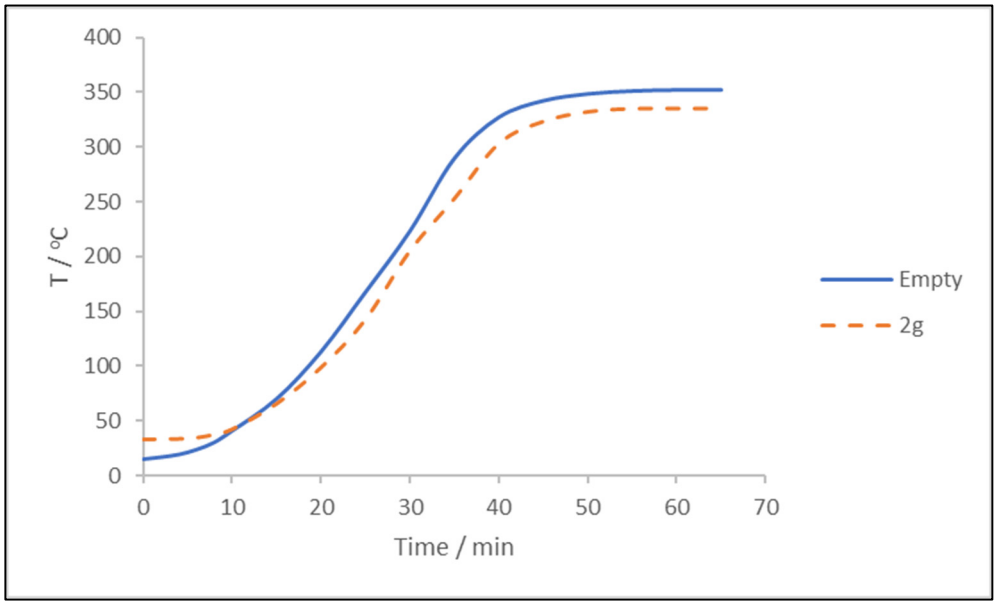

Figure 9. Temperature profile inside the reactor when empty and with 2 g of biomass.

From these two sets of data, and using Equation (4), the heat flow corresponding to the heat absorbed by the sample during the torrefaction process was estimated as a function of time. The results, for three different amounts of biomass in the reactor, are depicted in Figure 10.

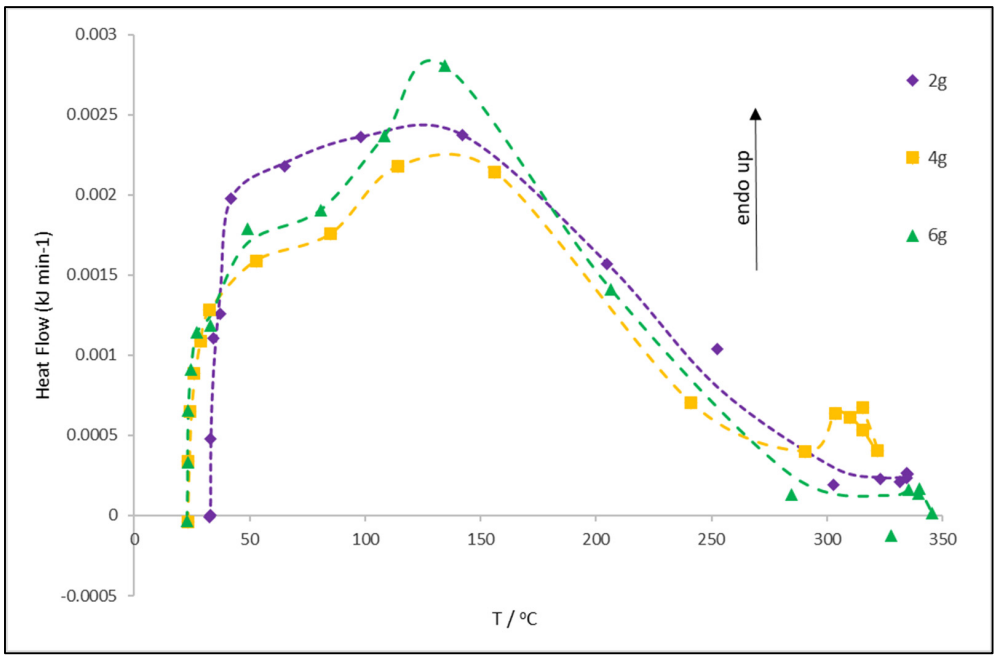

Figure 10. Computed heat flow on the lab-scale reactor for 30 min torrefaction of *Cistus ladanifer* biomass at 350 °C (symbols—experimental results, dashed line—trend line). The trend line was added for visualization purposes only and does not correspond to a model.

It can be seen that the majority of the heat requirements occurs up to around 140 °C, and it corresponds mostly to water release, through evaporation, and also through the decomposition of cellulose and hemicelluloses.

The total amount of energy that is transferred to the reactor for the process can be obtained by integrating the heat flow into the reactor. For example, processing 2, 4, and 6 g

in the reactor leads to an overall energy transferred to the reactor (corresponding to the integral of the curve shown in Figure 10) of 0.22, 0.10, and 0.07 MJ/Kg, respectively. This is the energy that is supplied and compares favourably with the outcome of 10 MJ/Kg of torrefied charcoal.

3.6. Structural Observations

SEM analysis was performed to evaluate the morphological changes on the lignocellulosic structure of each torrefied solid at 250 °C and 350 °C for 30 min and to compare them with raw biomass. After the torrefaction process, the torrefied biomass became darker and more brittle as the temperature increased. Figure 11 shows the impact of torrefaction temperature on the microscopic structure of torrefied solids.

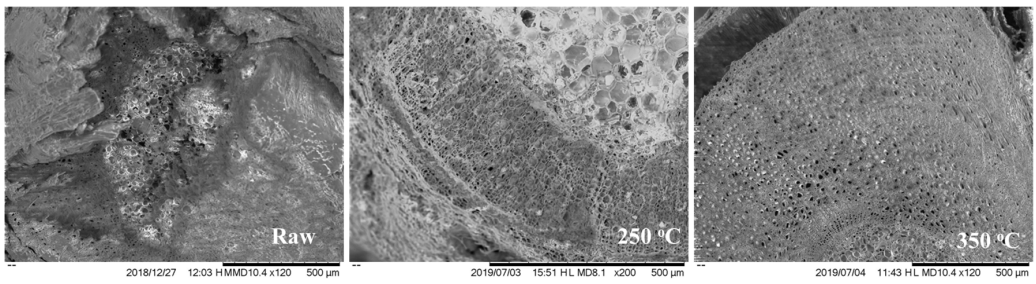

Figure 11. SEM images of raw and torrefied material.

From the cross-sectional images, it is clear that with the increase in temperature of torrefaction, the wood cell structure is still well defined with micropores given by the cell lumen distributed throughout the surface. This indicates that the cell structure was maintained, with the evaporation of intracellular water and the release of the more volatile components, leaving the lumen voids that correspond to the charcoal micropores. These micropores seem to be more or less regularly distributed in the material following its original cellular arrangement and are clearer in the sample torrefied at higher temperature. Downie and co-workers reported that the temperature increase can result in an enhancement of char micropore development to some extent [36].

These changes are also in line with observations from other researchers [37–39] who generally attribute them to the devolatilization and depolymerization of biomass, releasing volatiles and rearranging cellular structures [40,41].

4. Conclusions

These results indicate that the torrefaction of *Cistus ladanifer* is a promising technique for the energy densification of biomass. The overall energy balance is positive, with much lower energy requirements in comparison with the energy that can be obtained from the charcoal that is produced. The amount of energy that was necessary to supply to the lab-scale reactor during the torrefaction process was only 0.06 MJ/kg, a value that was possible to obtain through the development of a simple but innovative model to the reactor itself that allowed us to analyse the thermal behaviour of the reactor even in unsteady-state operation. This value compares favourably with the 10 MJ/kg that can be obtained through burning of the torrefied charcoal. The findings obtained in this work also indicated that torrefaction of *Cistus ladanifer* shrub biomass is a good approach to significantly reduce the mass and volume of the material while maintaining and, sometimes, even increasing its energy content relative to the original biomass, which is a novel observation and means that the torrefaction process is actually acting as energy storage, something that would be particularly significant if solar energy is used in the torrefaction. This will allow for more economic transportation of the biomass, in particular if the torrefaction process is carried out close to the collection site in a mobile system. It will also allow its more efficient further usage, either directly in power plants, in domestic applications, for further processing in

gasification, or even in soil amendment. The charcoal that is produced may also contribute to wastewater treatment, since the charcoal produced can assist in water filtration.

The results also indicate that the torrefaction process is effective even if the samples are not crushed prior to torrefaction, which is particularly relevant if the operation is to be carried out in the field. Also relevant is the fact that using different amounts of biomass in the reactor did not show significant differences in the behaviour and increasing the amount of biomass in the reactor is not deleterious to the process, a fact that, again, will be very important for practical application in a non-conventional torrefaction process, for example, in mobile equipment. It is also important to remember that crushing after torrefaction is also expected to be less energy consuming as torrefied biomass is more friable than the original biomass.

From all these observations, we believe that these studies will help in designing a mobile system that can travel through the forest areas and proceed, on site, to the torrefaction of forest residues for later transport to units that can use the charcoal as a fuel.

The development of a combined kinetic model for the description of the thermochemical decomposition of biomass during pyrolysis and combustion reactions is important to the understanding of biomass behaviour. The results obtained showed that the model was well described by five pseudo-components and ash.

As a future prospective, the gaseous products of the pyrolysis process can be evaluated to quantify their capacity, in terms of burning characteristics, to feed the torrefaction process and to be able to design combustion equipment, although preliminary results do not show this to be an effective way to provide heat to the system. An energy balance to evaluate the benefit of torrefaction through the relationship between the energy expenditure to produce torrefied biomass and the energy contained in it, should be addressed.

Author Contributions: Methodology—design and supervision, M.A.L., F.L. and H.P.; investigation, M.M.; resources, M.A.L. and F.L.; writing—original draft preparation, M.M.; writing—review, M.A.L., F.L. and H.P. All authors have read and agreed to the published version of the manuscript.

Funding: This research was funded by the College of Chemistry of the University of Lisbon through the Ph.D. grant (Ref. 14/BD/2017) to the first author and by Fundação para a Ciência e a Tecnologia to the project UIDB/04028/2020 (CERENA).

Data Availability Statement: The data presented in this study are available on request from the corresponding author. The data are not publicly available due to privacy policy.

Acknowledgments: The author would like to thank the financial support from the College of Chemistry of the University of Lisbon (CQUL) for the Ph.D. grant (Ref. 14/BD/2017) and to the project UIDB/04028/2020 (CERENA). The authors would also like to thank Teresa Quilhó and Isabel Miranda from the School of Agriculture of the University of Lisbon, for the support given in sample procurement and characterization.

Conflicts of Interest: The authors declare no conflict of interest.

References

1. Eurostat Statistics Expalined. Available online: https://ec.europa.eu/eurostat/statistics-explained/index.php?title=Energy_production_and_imports#Production_of_primary_energy_decreased_between_2008_and_2018 (accessed on 14 July 2023).
2. Zhang, S.; Zou, K.; Li, B.; Shim, H.; Huang, Y. Key Considerations on The Industrial Application of Lignocellulosic Biomass Pyrolysis toward Carbon Neutrality. *Engineering* **2023**, *29*, 35–38. [CrossRef]
3. Ferreira, S.; Monteiro, E.; Brito, P.; Vilarinho, C. Biomass resources in Portugal: Current status and prospects. *Renew. Sustain. Energy Rev.* **2017**, *78*, 1221–1235. [CrossRef]
4. Chen, W.-H.; Peng, J.; Bi, X.T. A state-of-the-art review of biomass torrefaction, densification and applications. *Renew. Sustain. Energy Rev.* **2015**, *44*, 847–866. [CrossRef]
5. Li, B.; Tang, J.; Xie, X.; Wei, J.; Xu, D.; Shi, L.; Ding, K.; Zhang, S.; Hu, X.; Zhang, S.; et al. Char structure evolution during molten salt pyrolysis of biomass: Effect of temperature. *Fuel* **2023**, *331*, 125747. [CrossRef]
6. Medic, D.; Darr, M.; Shah, A.; Potter, B.; Zimmerman, J. Effects of torrefaction process parameters on biomass feedstock upgrading. *Fuel* **2012**, *91*, 147–154. [CrossRef]
7. Ribeiro, J.M.C.; Godina, R.; Matias, J.C.O.; Nunes, L.J.R. Future Perspectives of Biomass Torrefaction: Review of the Current State-Of-The-Art and Research Development. *Sustainability* **2018**, *10*, 2323. [CrossRef]

8. Stelt, M.J.C.V.; Gerhauser, H.; Kiel, J.H.A.; Ptasinski, K.J. Biomass upgrading by torrefaction for the production of biofuels: A review. *Biomass Bioenergy* **2011**, *35*, 3748–3762.
9. Cahyanti, M.N.; Doddapaneni, T.R.K.C.; Kikas, T. Biomass torrefaction: An overview on process parameters, economic and environmental aspects and recent advancements. *Bioresour. Technol.* **2020**, *301*, 122737. [CrossRef]
10. Yan, W.; Acharjee, T.C.; Coronella, C.J.; Vasquez, V.R. Thermal pretreatment of lignocellulosic biomass. *Environ. Prog. Sustain. Energy* **2009**, *28*, 435–440. [CrossRef]
11. Martins, M.; Lemos, M.A.; Lemos, F.; Pereira, H. Solid Fuels Production from Forestry wastes using slow pyrolysis. In Proceedings of the 27th European Biomass Conference and Exhibition, Lisboa, Portugal, 27–30 May 2019; pp. 1185–1190.
12. Chen, J.J.; Doshi, V. Recent Advances in biomass pretreatment-torrefaction fundamentals and technology. *Renew. Sustain. Energy Rev.* **2011**, *15*, 4212–4222.
13. Rousset, P.; Aguiar, C.; Labbe, N.; Commandre, J.M. Enhancing the combustible properties of bamboo by torrefaction. *Bioresour. Technol.* **2011**, *102*, 8225–8231. [CrossRef] [PubMed]
14. *TAPPI T 211 om-02*; Ash in Wood, Pulp, Paper, and Paperboard: Combustion at 525 °C. TAPPI Test Methods. TAPPI Press: Atlanta, GA, USA, 2002.
15. *TAPPI T 204 cm-97*; Solvent Extractives of Wood and Pulp. Tappi Test Methods. TAPPI Press: Atlanta, GA, USA, 1997.
16. *TAPPI T 222 om-02*; Acid-Insoluble Lignin in Wood and Pulp. TAPPI Test Methods. TAPPI Press: Atlanta, GA, USA, 2002.
17. *TAPPI UM-250*; Acid-Soluble Lignin in Wood and Pulp. TAPPI Useful Method. TAPPI Press: Atlanta, GA, USA, 1991.
18. Ferreira, J.A.; Miranda, I.; Duarte, L.C.; Roseiro, L.B.; Lourenço, A.; Quilhó, T.; Cardoso, S.; Fernandes, M.C.; Carvalheiro, F.; Pereira, H. *Cistus Ladanifer* as source of chemicals: Structural and chemical characterization. *Biomass Conv. Bioref.* **2020**, *10*, 325–337. [CrossRef]
19. Martinez, M.G.; Dupont, C.; Perez, D.S.; Rodriguez, L.M.; Grateau, M.; Thiéry, S.; Tamminen, T.; Meyer, X.-M.; Gourdon, C. Assessing the suitability of recovering shrub biowaste involved in the South of Europe through torrefaction mobile units. *J. Environ. Manag.* **2019**, *236*, 551–560. [CrossRef]
20. Chen, W.-H.; Lin, B.-J.; Lin, Y.-Y.; Chu, Y.-S.; Ubando, A.T.; Show, P.L.; Ong, H.C.; Chang, J.-S.; Ho, S.-H.; Culaba, A.B.; et al. Progress in biomass torrefaction: Principles, applications and challenges. *Prog. Energy Combust. Sci.* **2021**, *82*, 100887. [CrossRef]
21. Amutio, M.; Lopez, G.; Alvarez, J.; Moreira, R.; Duarte, G.; Nunes, J.; Olazar, M.; Bilbao, J. Pyrolysis kinetics of forestry residues from the Portuguese Central Inland Region. *Chem. Eng. Res. Des.* **2013**, *91*, 2682–2690. [CrossRef]
22. Yang, H.; Yan, R.; Chen, H.; Lee, D.H.; Zheng, C. Characteristics of hemicellulose, cellulose and lignin pyrolysis. *Fuel* **2007**, *86*, 1781–1788. [CrossRef]
23. Bryś, A.; Ostrowska-Ligęza, E.; Bryś, J.; Górnicki, K. Wood biomass characterization by DSC or FT-IR spectroscopy. *J. Therm. Anal. Calorim.* **2016**, *126*, 27–35. [CrossRef]
24. Kopczyński, M.; Plis, A.; Zuwała, J. Thermogravimetric and Kinetic Analysis of Raw and Torrefied Biomass Combustion. *Chem. Process. Eng.* **2015**, *36*, 209–223. [CrossRef]
25. Mukhtara, H.; Feroze, N.; Munir, H.M.S.; Javed, F.; Kazmi, M. Torrefaction process optimization of agriwaste for energy densification. *Energy Sources Part A Recovery Util. Environ. Eff.* **2019**, *42*, 2526–2544. [CrossRef]
26. Bergman, P.C.A.; Boersma, A.R.; Kiel, J.H.A.; Prins, M.J.; Ptasinski, K.J.; Janssen, F.J.J.G. *Torrefaction for Entrained-Flow Gasification of Biomass*; Report ECN-C-05-067; Energy Research Centre of the Netherlands: Petten, The Netherlands, 2005.
27. Cardona, S.; Gallego, L.J.; Vallencia, V.; Martinez, E.; Rios, L.A. Torrefaction of eucalyptus-tree residues: A new method for energy and mass balances of the process with the best torrefaction conditions. *Sustain. Energy Technol. Assess.* **2019**, *31*, 17–24. [CrossRef]
28. Phanphanich, M.; Mani, S. Impact of torrefaction on the grindability and fuel characteristics of forest biomass. *Bioresour. Technol.* **2011**, *102*, 1246–1253. [CrossRef] [PubMed]
29. Sadaka, S.; Negi, S. Improvements of biomass physical and thermochemical characteristics via torrefaction process. *Environ. Progress. Sustain.* **2009**, *28*, 427–434. [CrossRef]
30. Chen, W.H.; Hsu, H.C.; Lu, K.M.; Lee, W.J.; Lin, T.C. Thermal pretreatment of wood (Lauan) block by torrefaction and its influence on the properties of the biomass. *Energy* **2011**, *36*, 3012–3021. [CrossRef]
31. Niu, Y.; Lv, Y.; Lei, Y.; Liu, S.; Liang, Y.; Wang, D.; Hui, S. Biomass torrefaction: Properties, applications, challenges, and economy. *Renew. Sustain. Energy Rev.* **2019**, *115*, 109395. [CrossRef]
32. Wang, L.; Barta-Rajnai, E.; Skreiberg, Ø.; Khali, R.; Czégény, Z.; Jakab, E.; Barta, Z.; Grønli, M. Effect of torrefaction on physiochemical characteristics and grindability of stem wood, stump, and bark. *Appl. Energy* **2018**, *227*, 137–148. [CrossRef]
33. Almeida, G.; Brito, J.O.; Perre, P. Alterations in energy properties of eucalyptus wood and bark subjected to torrefaction: The potential of mass loss as a synthetic indicator. *Bioresour. Technol.* **2010**, *101*, 9778–9784. [CrossRef] [PubMed]
34. Rodrigues, A.; Loureiro, L.; Nunes, L.J.R. Torrefaction of woody biomasses from poplar SRC and Portuguese roundwood: Properties of torrefied products. *Biomass Bioenergy* **2018**, *108*, 55–65. [CrossRef]
35. Basu, P. *Biomass Gasification, Pyrolysis, and Torrefaction: Practical Design and Theory*, 2nd ed.; Academic Press: Cambridge, MA, USA, 2013.
36. Downie, A.; Crosky, A.; Munroe, P. Physical Properties of Biochar. In *Biochar for Environmental Management: Science and Technology*; Lehmann, J., Joseph, S., Eds.; Earthscan: London, UK, 2009; pp. 13–32.
37. Li, X.; Bian, J. Effect of temperature and holding time on bamboo torrefaction. *Biomass Bioenergy* **2015**, *83*, 366–372. [CrossRef]

38. Park, J.; Meng, J.; Lim, K.H.; Rojas, O.J.; Park, S. Transformation of lignocellulosic biomass during torrefaction. *J. Anal. Appl. Pyrol.* **2013**, *100*, 199–206. [CrossRef]
39. Chen, W.-H.; Lu, K.-M.; Tsai, C.-M. An experimental analysis on property and structure variations of agricultural wastes undergoing torrefaction. *Appl. Energy* **2012**, *100*, 318–325. [CrossRef]
40. Shang, L.; Ahrenfeldt, J.; Holm, J.K.; Sanadi, A.R.; Barsberg, S.T.; Thomsen, T.S.; Wolfgang, H.; Henriksen, B.U. Changes of chemical and mechanical behavior of torrefied wheat straw. *Biomass Bioenergy* **2012**, *40*, 63–70. [CrossRef]
41. Sarker, T.; Azargohar, A. Physicochemical and Fuel Characteristics of Torrefied Agricultural Residues for Sustainable Fuel Production. *Energy Fuels* **2020**, *34*, 14169–14181. [CrossRef]